

CERIUM SUPPORTED ON HIGH POROUS CARBON FROM FISH SCALES CARP, AS A NOVEL LOW COST ADSORBENT TO REMOVE As(V) IONS FROM WATER

Zlate S. Veličković^{1*}, Radovan Karkalić¹, Zoran J. Bajić¹, Aleksandar D. Marinković², Aleksandar Nikolić³, Pavel Otřísal⁴, Stanislav Florus⁴

¹Military Academy, University of Defence of Belgrade, 33 Generala Pavla Jurišića Šturma str., 11000 Belgrade, Serbia

²Faculty of Technology and Metallurgy, University of Belgrade, 4 Karnegijeva, 11000 Belgrade

³Faculty of chemistry, University of Belgrade, 12-16 Studentski trg, 11000 Belgrade, Serbia

⁴University of Defence, NBC Defence Institute, Víta Nejedlého, 682 01 Vyškov, Czech Republic

Abstract

A novel, low cost adsorbent, a cerium supported on high porous carbon from fish scales carp (Cyprinus carpio), has been synthesized to remove As(V) ions from water. The synthesis consisted of chemical and thermal treatment for converting the fish scales into the porous carbon decorated by cerium nanoparticles. By changing the reaction conditions, the porosity and the content of the CeO₂ nanoparticles may be controlled in synthesized porous carbon. By optimizing the reaction parameters, using the response surface methodology (RSM) where the output is the result of the adsorbent capacity, a highly efficient material (CeO₂-HPC) with a capacity of 81.664 mg g⁻¹ (Langmuir isothermal model) was obtained to remove As (V) ions from the drinking water. The adsorption studies were conducted as a function of pH, contact time, mass of adsorbent and temperature. The best sorption of arsenate ions was achieved for pH between 4.0 and 6.0. The adsorption data for arsenate at 25, 35 and 45 °C are fitted to Langmuir, Freundlich, Dubinin-Radushkevich (D-R) and Temkin isotherm models. Experimental data were used to model adsorption kinetics using pseudo-first order, pseudo-second order, Elovich and intraparticle diffusion kinetic models. The results showed that the adsorption of As(V) ions onto CeO₂-HPC followed the pseudo-second-order kinetic model and Freundlich isotherm models. Thermodynamic parameters, including the Gibbs free energy (ΔG^0), enthalpy (ΔH^0), and entropy (ΔS^0) changes, indicated that the present adsorption process was feasible, spontaneous and endothermic in the temperature range of 25-45 °C.

Keywords: arsenate, adsorption isotherms, drinking water, carp scale, CeO₂ nanoparticles

1. INTRODUCTION

Arsenic is a metalloid occurring in the form of minerals located in the earth's crust and naturally existing in groundwater. However, numerous human activities (industry, agriculture, energy) contribute to the growing contamination of arsenic of surface and groundwater. Arsenic water pollution is a problem of many parts of the world including the northern parts of Serbia. Arsenic has been classified by the World Health Organization (WHO) in group A of carcinogens. Back in 1993 the maximum allowed contamination in drinking water has been revised and changed from 50 to 10 µg L⁻¹. This low restrictive limit for arsenic in drinking water has sparked extensive research and development of new technologies and materials for its removal from water. However, to date, a widely applicable, commercially acceptable method for the removal of arsenic, especially at lower concentrations, has not been developed. The researchers' attention has been recently attracted with the use of cheap, widespread materials such as clay, zeolite and tuff (Bajić et al. 2013, 2016), various metals and their oxides in conventional and nanostructural form of goethite, magnetite, alumina and waste materials from industry and agriculture, such as flying ash, slag, waste PAN fibers, fish scales, cellulose, etc.

In this study the possibility of using cerium supported on high porous carbon from carp fish scales (Cyprinus carpio) for the removal of As(V) ions from aqueous solution was investigated.

Because of the availability of the material in large quantity, the scales are at the moment considered only as a bio waste (Bajić et al. 2013, 2016), and the development of the technology for the hazardous material removal from water provide multiple contribution to environmental protection.

In this study, we report for the first time that fish scales can be an excellent raw material for synthesizing highly porous cerium supported carbon for As(V) ion adsorption, with the following advantages. First, protein is the main component of fish scales, containing both carbon and nitrogen. Second, hydroxyapatite, which exists in fish scales on the nanoscale, could be used as a natural template for porous carbon synthesis. Third, fish scales are an inexpensive by-product of the food processing industry. The results show that the synthesized a cerium supported on high porous carbon has a very high specific surface area of $1067 \text{ m}^2 \text{ g}^{-1}$ and large pore volume (total pore volume up to $0.638 \text{ cm}^3 \text{ g}^{-1}$). More importantly, this carbon exhibits strong removal capacity for As(V) ions, up to 81.664 mg g^{-1} at $45 \text{ }^\circ\text{C}$, and is a promising adsorbent for removal As(V) ion for drink water.

2. MATERIALS AND METHODS

2.1. Materials

During the experimental part of this survey a great number of chemicals and reagents are used. Bearing in mind that the properties of the adsorbent, the reproducibility of the synthesis and adsorption results largely depend on the purity of the reagents, high purity chemicals were used:

- Cerium(III) chloride heptahydrate - $\text{CeCl}_3 \times 7\text{H}_2\text{O}$ (Sigma Aldrich, PA), was used in the procedure of supported cerium nanoparticles from fish scale,
- 5% solution of hydrogen peroxide H_2O_2 (Sigma-Aldrich, PA),
- concentrated nitric acid HNO_3 (Fluka, ultrapure), was used for the preparation of a solution for adjusting the pH of the digestion and adsorbents in the process of determining the content of the present elements,
- sodium hydroxide - NaOH (Sigma Aldrich, PA), was used for preparing a solution for adjusting the pH value of the solution of arsenic in the process of supported cerium nanoparticles from fish scale,
- potassium hydroxide - KOH (Sigma Aldrich, PA), was used to activate carbon during carbonization,
- Deionized water (DI) (a resistance of $18 \text{ M}\Omega \text{ cm}$) was used for preparation of samples and the rinsing solution,
- $\text{Na}_2\text{HAsO}_4 \cdot 7\text{H}_2\text{O}$ (Sigma-Aldrich). Stock solutions containing 1000 mg dm^{-3} were prepared, and additionally diluted with DI water to the required concentrations for the adsorption experiments.
- fish scales were collected from farmed carp (*Cyprinus carpio*), grown in Ečka fish farm, Serbia,

2.2. Adsorbent synthesis

The fish scales were collected from farmed carp (*Cyprinus carpio*), grown in Ečka fish farm, Serbia. Scales were sonicated in a 5% solution of hydrogen peroxide and triple rinsed in with deionized (DI) water and dried. Pure dried carp scales (PCS) were grinded and sieved to obtain material with narrower distribution of $100 \pm 50 \mu\text{m}$ grain. The highly porous cerium nanoparticles-doped carbon was prepared as follows: 1 g PCS were dispersed into 20 mL distilled water and agitated with a magnetic agitator. The $\text{CeCl}_3 \times 7\text{H}_2\text{O}$ ($0.08 \text{ g mL}^{-1} \approx 0.03 \text{ g Ce mL}^{-1}$) solution was added into the PCS solution drop by drop. After the mixture was agitated for 1 h, 0.5 wt.% NaOH was titrated into the mixture until the pH value reaches 9.

The mixture was then dried up and heated in the atmosphere of nitrogen at $330 \text{ }^\circ\text{C}$ for 3 h to oxidize $\text{Ce}(\text{OH})_3$ particles to CeO_2 nanoparticles. The precarbonized fish scales were then blended with KOH (as an activating agent) in a weight ratio of 1:1 and ground to powder. The powder was heated in a N_2

atmosphere at different temperatures (in the range of 600–900 °C). The highly porous cerium nanoparticles supported on high porous carbon (Ce-HPC) can be prepared.

2.3. Optimization of adsorbent preparation

The optimization of the ratio of the initial amount of CeCl_3 and the carbonization temperature of the cerium nanoparticles supported PCS was performed with the intent to obtain a high performance adsorbent used to remove ion As(V) from the water.

As the most influential working parameters in the synthesis of adsorbents based on PCS and cerium nanoparticles, the initial amount of Ce in the reaction mixture and the carbonization temperature were selected in the optimization process to achieve the goals of optimizing the high adsorption capacity. Optimization of the adsorption synthesis was carried out using the surface response methodology (RSM), based on two factors D-optimal design. RSM is in compliance with the principles of environmental protection, where there is a significant decrease in the number of experiments, and consequently a decrease in waste production. The operational values of the selected variables in the experimental plan are given in Table 1, which includes 13 experimental papers with five replications at the center point.

Run	V_{CeCl_3} (ml)	T (°C)	Response q_e (mg g ⁻¹)
1	3	750	53.80
2	3	600	34.22
3	1	750	25.35
4	5	750	45.33
5	3	750	53.80
6	5	600	25.11
7	3	750	53.80
8	3	900	47.20
9	5	900	44.42
10	1	900	18.00
11	1	600	22.20
12	3	750	53.80
13	3	750	53.80

Table 1. Experimental plan two factor Optimal (custom) Design of the adsorption capacity of CeO_2 -HPC in relation to the volume of the CeCl_3 constant concentration and the carbonization temperature of the CeO_2 - PCS

Each experiment (except the central point) was performed in duplicate. The output variable was the adsorption capacity. The data obtained in these experiments were fitted with a second-order polynomial equation and the coefficients of the response function and their statistical significance were evaluated by the least square method, using commercial software Design-Expert, Software Version 9 (Stat-Ease, Inc. 2021 E. Hennepin Ave. Suite 480 Minneapolis, USA).

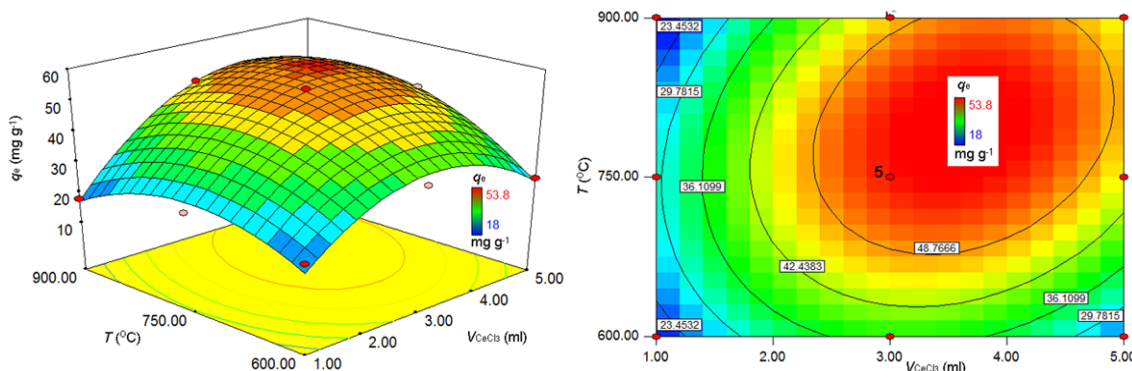


Fig. 1. The estimated surface (a) and contour (b) plots based on q_e (mg g^{-1}) for As(V) ions [$C_{i \text{ As(V)}} = 5.78 \text{ mg dm}^{-3}$, $m_{\text{ads}} = 2 \text{ mg}$, $V = 10 \text{ ml}$, $t = 240 \text{ min}$ and $\text{pH} = 6$]

2.4. Methods of material characterization

CeO₂-HPC adsorbent is characterized by using FTIR and the BET techniques, and the zeta potential was also determined.

Specific surface area, specific pore volume and pore diameter were determined by BET nitrogen adsorption / desorption at 77.4 K, using a gas sorption analyzer Micromeritics ASAP 2020MP v 1.05 H.

IR spectra of the Fourier Transform - (FTIR) spectra were recorded in transmission mode between 400 and 4000 cm^{-1} , at a resolution of 4 cm^{-1} using a Bomem spectrometer (Brown & Hartmann).

Zeta potential analyzer (Zetasizer 2000, Malvern, UK) was used for determining the zeta potential of adsorbents. The pH value of the point of zero charge (pH_{pzc}) the samples were determined by "drift" method [3].

2.5. Conditions and procedure for adsorption As(V) ion on the CeO₂-HPC

Adsorption experiments were carried out in batch conditions, with the initial concentration of As(V) solutions ($C_0 = 5.78 \text{ mg L}^{-1}$) and adsorbent masses of 100 to 500 mg L^{-1} . In order to investigate the effects of pH on the adsorption of As(V) ions, the initial pH value of the solution was varied between 4.0 and 12.0. Thermodynamic adsorption experiments were performed at 25, 35 and 45 °C. The effect of contact time on the adsorption of ions As(V) was monitored over a period of 10-90 minutes. The amount of adsorbed ions is calculated from the difference between the initial and the equilibrium concentration.

The results were analyzed using the normalized standard deviation Δq (%), which is calculated by the following equation:

$$\Delta q(\%) = \sqrt{\sum \frac{[(q_{\text{exp}} - q_{\text{cal}}) / q_{\text{exp}}]^2}{N - 1}} \times 100 \quad (1)$$

where q_{exp} and q_{cal} are the experimental and the calculated amount of As(V) ions adsorbed on CeO₂-HPC, N is the number of data used in the analysis. All experiments were repeated three times, and only their mean values are given. The maximum deviation is < 3% (experimental error). All calculated standard errors for isotherm parameters, kinetic and thermodynamic parameters were determined using commercial software (Microcal Origin 8.0) in the linear regression program.

Concentration of As(V) ions were measured using the Agilent 7500C ICP-MS system (Agilent Technologies, Inc.).

3. RESULTS AND DISCUSSION

3.1. Physical and chemical characterization of the adsorbent

Surface properties and physical properties of the adsorbent are given in Table 2. The change of pH_{PZC} was influenced by the change of surface properties due to cerium nanoparticles deposition (Table 2). Low pH_{PZC} values of both adsorbent indicate that negatively charged surface, at $pH > pH_{PZC}$, could be a driving force due to higher contribution of electrostatic sorbate/adsorbent interaction. Also, increase of pH_{PZC} value after adsorption, indicates that contribution of specific adsorption, rather than electrostatic interactions, are the processes operative in the course of arsenic adsorption.

Adsorbent	Specific surface area ($m^2 g^{-1}$)	Pore volume ($cm^3 g^{-1}$)	Mean pore diameter (nm)	pH_{PZC}	Zeta potential (mV)
CeO ₂ -HPC	1067	0.638	2.5	6.84	-17.4 (pH 5.02)

Table 2. Physical properties of CeO₂-HPC

The arsenic removal mechanism was further investigated using the FTIR technique. FTIR spectra of the CeO₂-HPC and CeO₂-HPC /As(V) are shown in Figure 2. From the spectra it could be seen that before the arsenic adsorption (Fig. 2), the peak at 3418 cm^{-1} corresponds to the N–H stretching vibration, but it overlaps with O–H stretching vibration, making identification difficult. OH stretching and bending vibrations of surface adsorbed water at 1628 cm^{-1} along with Ce–OH bending vibrations at $1110, 1055, \text{ cm}^{-1}$, are present. (Sawana et al. 2017) The weak peak at 1720 cm^{-1} corresponds to the C=O stretching vibration. (Huang et al. 2015). The band at 1250 cm^{-1} is attributed to the C–N stretching vibration. The band 1490 cm^{-1} is attributable to the C–H bending vibrations of the CH₃ and CH₂ groups. The band at 550 cm^{-1} is from the Ce–O stretching vibrations of the coating (Duan et al. 2011; Lu et al. 2014). Finally the peak at $ca.700\text{ cm}^{-1}$ in corresponds to the vibrational stretching of the Ce–O–C bond (Periyat et al. 2011).

After the arsenic adsorption experiments (Fig. 2), the Ce–OH bending vibrations disappeared and a new vibration at 839 cm^{-1} appeared which could be attributed to m(As–O–Ce) bond. Appearance of this As–O–Ce vibration indicates that the adsorption of both As(V) follows the inner sphere mechanism. The FTIR studies indicate that the substitution of OH groups by As from Ce–OH plays a major role in the adsorption process which could also be explained through specific adsorption mechanism. The specific adsorption involves ligand exchange reactions where the anions displace OH⁻ and/or H₂O from the surface (Sawana et al. 2017).

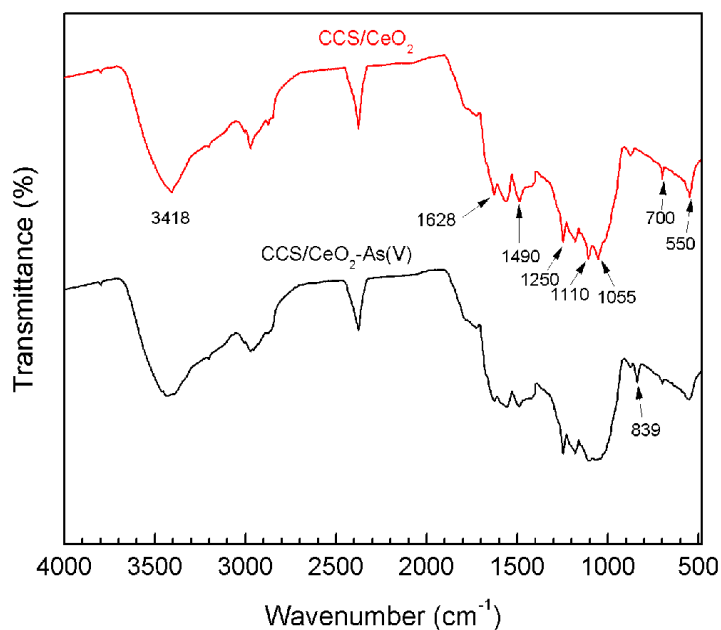


Fig 2. FTIR spectra of adsorbent CeO₂-HPC before (c) and after treatment with As(V) , [C₀= 5 mg dm⁻³, m/V = 1 mg ml⁻¹, pH = 6]

3.2. The effect of solution pH on the adsorption of the As(V)

The effect of pH on the sorption capacity of the CeO₂-HPC can be explained in terms of pHPZC. When pH < pHPZC the particle surface is positively charged (behave as Bronsted acids and anion exchangers). Thus, more favorable electrostatic attraction forces enhanced As(V) ion adsorption as pH increases.

CeO₂-HPC adsorbents, where an increasing negative surface potential at pH values greater than pHPZC (6.84) is due to deprotonation of hydroxyl groups present on the adsorbent surface. Improved textural parameters of CeO₂-HPC, *i.e.* increased specific surface area, indicates higher availability of surface active sites to increased capability of adsorbents for removal of arsenic.

Adsorption efficiency of As(V), ions on the adsorbent was studied at pH range between 4 and 12 (Figure 3). The pH value of the solution influences the surface charge of the adsorbent, the degree of ionization, the content of the metal species in the aqueous solutions and the surface properties of the adsorbent. It is known that speciation of heavy metals in the water depend on the pH value (Veličković et al. 2013), and different forms could exist arsenic in the form of H₃AsO₄, H₂AsO₄⁻, HAsO₄²⁻, AsO₄³⁻ species (Fig. 3).

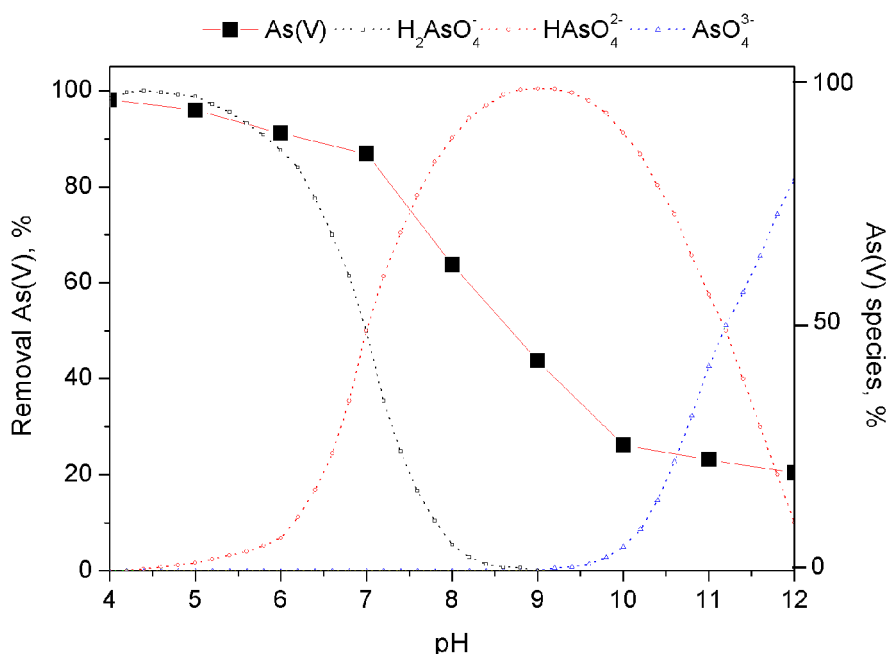


Fig. 3. Influence of pH on adsorption of As(V) ions on CeO₂-HPC $C_{[As(V)]_0} = 5.78 \text{ mg L}^{-1}$, $m/V = 500 \text{ mg L}^{-1}$, $T = 25 \text{ }^\circ\text{C}$

The adsorption of As(V) ions on the adsorbent CeO₂-HPC is more favorable at pH values lower than 6.84 pH_{PZC} . At $\text{pH}_i < \text{pH}_{\text{PZC}}$ the As(V) removal percentages was in the range 89.0 and 97.0%. The electrostatic interaction between the positively charged surface of the adsorbent and the negatively charged ionic species of arsenic, monovalent anion H₂AsO₄⁻ ($\text{pK}_{a1} = 2.3$), leads to more favorable adsorption (Veličković et al. 2012).

At higher pH the presence of divalent As(V) anion dominates in solution and repulsion with negative adsorbent surface cause lower adsorption efficiency. The pH change during adsorption is an indication that protonation/deprotonation reactions of surface functional group together with adsorption of arsenic species are operative (Veličković et al. 2012). It should be emphasized that even at $\text{pH} > \text{pH}_{\text{PZC}}$, arsenate adsorption occurs in certain extent, despite the repulsion between the present species and negative surface. Probably, during the formation of new bonds between surface and arsenate ions, repulsive forces are neutralized (Veličković et al. 2013).

3.3. The effect of the contact time on the adsorption of arsenate ions

The effect of time on the adsorption of arsenate ions was analyzed in the range from 10 to 90 minutes (Figure 4). Among two method used in an adsorption experiments the system stimulated by sonication showed higher efficiency than conventional mixing. The presence of an ultrasonic field increases the speed of the adsorption due to the reduced resistance to mass transfer. Ultrasonic waves and the bubbles caused by the side effects of cavitation in a solid (adsorbent) generate micro disturbances, thus reducing the boundary layer and increasing the efficiency of mass transfer. In fact, these increase the affinity of the adsorbate to the adsorbent. In this case here, ultrasound does not alter the process of adsorption nor shift the equilibrium to lower concentrations (Markovski et al. 2014).

The kinetic results (Figure 4) demonstrate that process was fast in the first 60 minutes for As(V) (86 %) ions, and adsorption rate substantially decrease in the period from 60 to 90 minutes. Percent of As(V) ions removal increase to 99.4 %. Equilibrium was established for 150 and 180 minutes of As(V) ions adsorption. From that point of view in further study 90 minutes was used in analysis of kinetic data.

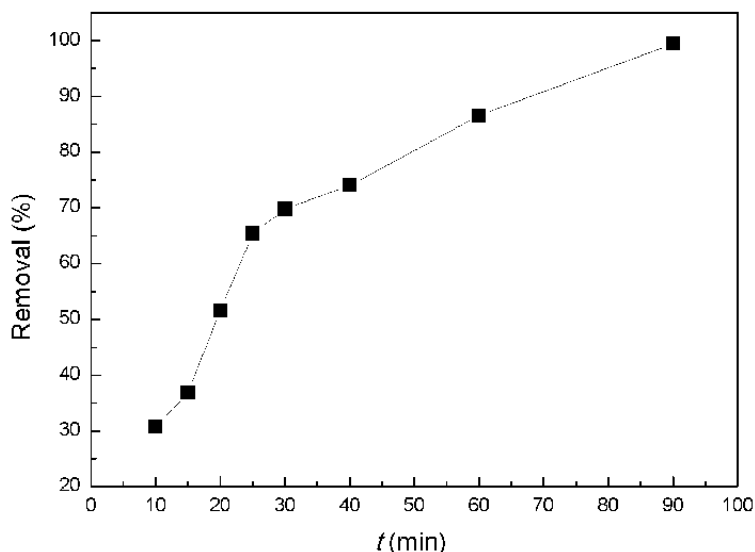


Fig. 4. Time dependent adsorption of As(V) onto CeO₂-HPC ($C_{i[AS(V)]} = 5.78 \text{ mg L}^{-1}$, pH = 4; $m/V = 500 \text{ mg L}^{-1}$, $T = 298 \text{ K}$)

3.4. Adsorption kinetics

In order to study the adsorption kinetics, the pseudo-first, pseudo-second-order and second order kinetic models were used (Bajić et al. 2016; Budimirović et al. 2017; Taleb et al. 2016a). According to the regression coefficient (r), as well as the Δq values and calculated standard error for all model parameters, the experimental kinetic data are better described using the pseudo-second order (PSO) equation (eq. (2)). An agreement of q_e values (Table 3) with the experimental results was obtained using PSO equation (2):

$$\frac{t}{q_t} = \frac{1}{K' q_e^2} + \frac{1}{q_e} t \quad (2)$$

Where q_e and q_t denote the amounts of adsorbed metal ions / mg g⁻¹ in equilibrium at certain time t , K' / g (mg min)⁻¹ is the pseudo-second order adsorption constant.

Adsorbate/order of kinetic law	Pseudo-first	Pseudo-second	Second order
q_e	15.741	16.026	16.026
As(V) $k(k_1, k_2)$	0.0677	0.002141	0.015358
R^2	0.983	0.982	0.992

Table 3. Kinetic parameters for As(V) adsorption onto CeO₂-HPC ($C_{i[AS(V)]} = 5.78 \text{ mg L}^{-1}$, pH = 4; $m/V = 500 \text{ mg L}^{-1}$, $T = 298 \text{ K}$)

Additionally, the rate controlling step of adsorption was evaluated using Weber-Morris model (W-M) (Budimirović et al. 2017). The model parameters are presented in Table 4.

Step	Constants	As(V)
Step 1	k_{p1} (mg g ⁻¹ min ^{-0.5})	1.945
(Intra-particle diffusion)	C (mg g ⁻¹)	-2.241
	R^2	0.997
Step 2	k_{p2} (mg g ⁻¹ min ^{-0.5})	0.775
(Equilibrium)	C (mg g ⁻¹)	3.342
	R^2	0.985

Table 4. The rate constants of intra-particle diffusion kinetic modeling ($C_{i[AS(V)]} = 5.78$ mg L⁻¹, pH = 4; $m/V = 500$ mg L⁻¹, $T = 298$ K)

The complex nature of the process of overall metal ions uptake was considered either by one general step, as it was described by PSO equation, or it could consecutive/competitive steps. The W–M fitting revealed that two successive linear steps describe adsorption process: fast kinetics in the first step and slower in second part. Overall ion transport was mainly controlled by intra-particle diffusion as indicated by larger intercept, i.e. constant C (Table 4). The first linear part describe external mass transfer to the adsorbent surface, while the second part describe the processes which take place in a porous structure of adsorbent, and strongly relate to pore geometry and network density of CeO₂-HPC. The intra-particle and film diffusion resistance slow down adsorbate transport, i.e. net transport in a direction of variable time-dependent concentration gradient. At the final stage of process, the adsorption takes place at low rate until saturation of all available surface sites is achieved (Bajić et al. 2016; Budimirović et al. 2017; Taleb et al. 2016 b).

3.5. Activation energy of the adsorption

According to the results of kinetic study performed at three temperature, i.e. 298, 308 and 318 K, it was possible to calculate activation energy according to Arrhenius equation. Plot describing the dependence of $\ln k$ versus $1/T$ (Kelvin degree) (Table 5).

Temperature	q_e (mg g ⁻¹)	k_2 (g (mg min) ⁻¹)	R^2
298 K	16.026	0.015358	0.992
308 K	36.491	0.015672	0.988
318 K	37.091	0.015991	0.992

Table 5. PSO model parameters for the adsorption of As(V) on CeO₂-HPC ($C_{i[AS(V)]} = 5.78$ mg L⁻¹, pH = 4; $m/V = 500$ mg L⁻¹)

The linear form of the Arrhenius equation is given by eq. (3):

$$\ln K' = -\frac{E_a}{RT} + \ln A \quad (3)$$

where K' is the reaction speed constant at the selected temperature, E_a denotes activation energy, R is a universal gas constant (8.314), T is the temperature in Kelvin, and A is the Arrhenius factor (frequency for the given reaction). The calculated results are as follows $E_a = 1.59$ kJ mol⁻¹. Magnitudes of the activation energy may assist in understanding the mechanism of the metal-ion adsorption on the adsorbent used. Physisorption or physical adsorption generally possesses activation energy 40 kJ mol⁻¹, while the chemisorption requires more energy and an activation energy above 40 kJ mol⁻¹ (Budimirović et al. 2017; Taleb et al. 2016a). According to this difference in activation energy, it can be concluded that the physisorption process was carried out in both cases. In practice, both physisorption and chemisorption can be expected on the adsorbent surface itself; for instance, the

molecule layer can be physically adsorbed on top of the basic chemisorbed layer (Budimirović et al. 2017).

3.6. Adsorption isotherm

The state of interaction/bonding on the solutes/adsorbent surface can be recorded by fitting experimental data with various adsorption isotherms. The normalized correlation coefficient and standard deviation were used here to evaluate the fitting of the adsorption data. The experimental data were compared to the models of the Langmuir, Freundlich, Temkin and Dubinin-Radushkevich isotherms utilized elsewhere in previous research within the literature (Bajić et al.2016; Budimirović et al. 2017; Taleb et al. 2016a), whose parameters are provided in Table 6. In order to determine the fit of the experimental data with the adsorption isotherm models, the normalized standard deviation Δq equation (1), together with the correlation coefficient R^2 were calculated. Analysis of the experimental data of As(V) adsorption on the adsorbent CeO₂-HPC indicate that the best fit of the data for an adsorbent according to the correlation coefficient is of a Freundlich-isotherm model. However, the Dubinin-Radushkevich isotherm is of the same coefficient of correlation, although it does possess a slightly lower normalized standard deviation. It can therefore be concluded that the Freundlich isotherm model better plots out the process for As(V) ions when using the CeO₂-HPC adsorbent. The best fitting of experimental data with isotherms model were given on Figure 5.

According to the Freundlich isotherm, the mechanism of As(V) ions adsorption onto CeO₂-HPC could be described by heterogenous adsorption, where the adsorbed ions/molecules had different enthalpies and adsorption activation energies. The n value from the Freundlich isotherm is a measure of the adsorption intensity or surface heterogeneity. Values of n close to zero indicate a highly heterogeneous surface. Value obtained of $n < 1$ (Table 6) implies chemisorption process, the higher value is an indication of cooperative adsorption, i.e., physisorption and chemisorption, with different contribution at different steps of the equilibration of the system (Taleb et al.2016 b).

Isotherm model and model parameters		Temperature		
		298 K	308 K	318 K
Langmuir isotherm	q_m (mg g ⁻¹)	78.616	79.882	81.644
	K_L (L mg ⁻¹)	4.865	4.858	4.836
	K_L (L mol ⁻¹)	364530	363981	363323
	R^2	0.980	0.977	0.967
Freundlich isotherm	K_F (mg g ⁻¹) (dm ³ mg ⁻¹) ^{1/n}	95.629	98.426	102.011
	$1/n$	0.600	0.606	0.613
	R^2	0.995	0.996	0.998
Temkin isotherm	A_T (dm ³ g ⁻¹)	53.090	53.606	54.519
	b_T	16.26	16.42	16.58
	B (kJ mol ⁻¹)	152.41	156.00	159.52
	R^2	0.969	0.965	0.957
Dubinin-Radushkevich isotherm	q_m (mg g ⁻¹)	59.48	60.00	60.35
	K_{ad} (mol ² kJ ⁻²)	7.14	7.13	7.12
	E_a (kJ mol ⁻¹)	8.369	8.374	8.377
	R^2	0.990	0.976	0.975

Table 6. Adsorption isotherm parameters for As(V) adsorption on the CeO₂-HPC ($C_{i[As(V)]} = 5.78$ mg L⁻¹, $m/V = 100 - 500$ mg L⁻¹, pH = 4)

The adsorption energy obtained from the Dubinin-Radushkevich isotherm may be a reliable indicator of the mechanism of adsorption on the adsorbent. If the value E_a is below 8 kJ mol^{-1} , the adsorption process can be considered to be physical adsorption. In contrast, if the value of E_a is in the range of $8 - 16 \text{ kJ mol}^{-1}$, it is a chemical adsorption. Table 6 notes that the obtained value of the mean free energy E_a , is in the range of $8.369 - 8.377 \text{ kJ mol}^{-1}$. Since E_a is close to the boundary, it can be concluded that both chemical and physical adsorption play a role in the adsorption of arsenate ion in the adsorbent (Budimirović et al. 2017).

The calculation of separation factor (R_L) according to eq. (4) based on Langmuir isotherm parameter b , indicate adsorption feasibility on the given adsorbent. It is calculated using the following equation (4):

$$R_L = \frac{1}{(1+bC_0)} \quad (4)$$

where C_0 (mol L^{-1}) is the initial adsorbate concentration and b (L mol^{-1}) is the Langmuir constant. The value of R_L points to the feasibility of adsorption process: irreversible ($R_L = 0$), favorable ($0 < R_L < 1$), linear ($R_L = 1$), unfavorable ($R_L > 1$). R_L for the adsorption of As(V) ions on $\text{CeO}_2\text{-HPC}$ is in the range from 0.0394 to 0.171 to be favorable (Bajić et al. 2016).

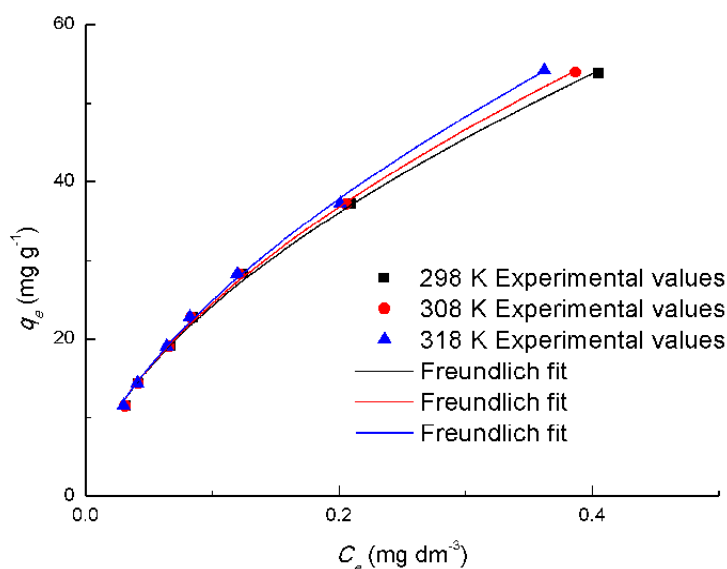


Fig. 5. The fitting of adsorption experimental data with Freundlich isotherm model adsorption of As(V) ions on $\text{CeO}_2\text{-HPC}$, $C_{i[\text{As(V)]}} = 5.78 \text{ mg L}^{-1}$, $m/V = 100 - 500 \text{ mg L}^{-1}$, $\text{pH} = 4$

Gibbs free energy (ΔG^0), enthalpy (ΔH^0) and entropy (ΔS^0) were calculated using Van't Hoff thermodynamic equations (5) and (6) (Veličković et al.2012):

$$\Delta G^0 = -RT \ln(b) \quad (5)$$

$$\ln(b) = \frac{\Delta S^0}{R} - \frac{\Delta H^0}{(RT)} \quad (6)$$

Where T is the absolute temperature in K, and R is the universal gas constant ($8.314 \text{ J mol}^{-1} \text{ K}^{-1}$) and the adsorption constant b was calculated using Langmuir isotherm (Table 7). ΔH^0 and ΔS^0 were calculated from slopes and interceptions in diagram $\ln(b) - T^{-1}$, assuming adsorption kinetics to be stationary (Veličković et al. 2012). The calculated thermodynamic parameters (Table 7) may cast light on the adsorption mechanisms of the studied ions on $\text{CeO}_2\text{-HPC}$.

Adsorbate	ΔG° (kJ mol ⁻¹)			ΔH° (kJ mol ⁻¹)	ΔS° (J mol ⁻¹ K ⁻¹)	R ²
	298 K	308 K	318 K			
As(V)	-42.51	-43.99	-45.56	2.93	152.38	0.939

Table 7. Calculated Gibbs free energy of adsorption, enthalpy and entropy for As(V) adsorption on CeO₂-HPC at 298, 308 and 318 K

The negative adsorption standard free energy changes (ΔG^0) and positive standard entropy changes (ΔS^0) at all temperatures indicates that the adsorption reactions are spontaneous (Table 7). The decrease of Gibbs free energy (ΔG^0) with increasing temperature indicates that spontaneity of the reaction increases. Regardless on coordination and hydrogen bonding, at higher temperature, solvated As(V) ion (Veličković et al. 2012) is more readily desolvated, diffusion through boundary layer and within the pores is a faster process, and adsorption processes become more favorable.

The positive values of ΔS^0 indicates a higher disorder tendency at the interface between CeO₂-HPC surface and As(V) solutions. This is presumably due to the increase of released solvent molecules when solvated solute distributes on the solid phase from the aqueous solution and the number of molecules increases at the solid-liquid interface. The results obtained are found to be similar to those that had been reported previously (Veličković et al. 2012). However, some processes like ion-exchange release ions from the solid surface into bulk solution and increase overall entropy of the system.

Regardless of the coordination properties, the solvated As(V) were more easily desolvated at higher temperatures, where the diffusion through the boundary layer and inside the pores occur at a higher diffusional rate. Generally, the change of free energy in the case of physisorption was recorded to be between -20 and 0 kJ mol⁻¹, for both physisorption and chemisorption between -20 and -80 kJ mol⁻¹. Therein, the interaction between As(V) and CeO₂-HPC of the combined physisorption and the chemisorption processes.

4. CONCLUSION

In the present work, the highly efficient low cost adsorbent, a cerium supported on high porous carbon from fish scales carp (*Cyprinus carpio*), has been synthesized to remove As(V) ions from water. The best adsorption performance of CeO₂-HPC was discussed as a consequence of the adsorbent specific surface area, mesopore volume and diameter, as well as of their hybrid nature. The use of adequate statistical analysis and proper selection of the isotherm model, i.e., Freundlich and Dubinin-Radushkevich models, led to the best correlation of the adsorption data. The best fitting of the kinetic data was obtained by the use of pseudo-second-order and Weber–Morris kinetic models, which showed that the intra-particle diffusional transport is a limiting step. The thermodynamic parameters revealed that the adsorption processes were favorable and more spontaneous at a higher temperature.

Adsorption of As(V) in the investigated adsorbent CeO₂-HPC is complex and probably involves physisorption and chemisorption mechanism. Arsenic ion adsorption capacity and affinity of the CeO₂-HPC groups depends on the surface, the pH, temperature, specific surface area, pore volume and diameter.

ACKNOWLEDGMENTS

The authors acknowledge financial support from Ministry of Education, Science and Technological development of the Republic of Serbia, Project No. 172057, and University of Defence, Republic of Serbia, project VA-TT/4/16-18.

REFERENCES

1. Bajić, ZJ, Djokić, VR, Veličković, ZS, Vuruna, MM, Ristić, MĐ, Issa, NB, Marinković, AD, 2013, `Equilibrium, kinetic and thermodynamic studies on removal of Cd(II), Pb(II) and As(V) from wastewater using carp (*cyprinus carpio*) scales`, *Dig. J. Nanomater. Biostruct.* vol. **8**, pp. 1581-1590.
2. Bajić, ZJ, Veličković, ZS, Djokić, VR, Perić-Grujić, AA, Ersen, O, Uskoković, PS & Marinković, AD, 2016, `Adsorption Study of Arsenic Removal by Novel Hybrid Copper Impregnated Tufa Adsorbents in a Batch System`, *Clean - Soil, Air and Water*, vol. 44, no. 11, pp. 1477-1488;
3. Budimirović, D, Veličković, ZS, Djokić, VR, Milosavljević, M, Markovski, J, Lević, S & Marinković, AD, 2017, `Efficient As(V) removal by α -FeOOH and α -FeOOH/ α -MnO₂ embedded PEG-6-arm functionalized multiwall carbon nanotubes`, *Chem. Eng. Res. Des.*, vol. 119, pp. 75–86.
4. Duan, W, Xie, A, Shen, Y, Wang, X, Wang, F, Zhang, Y & Li, J 2011, `Fabrication of Superhydrophobic Cotton Fabrics with UV Protection Based on CeO₂ Particles`, *Ind. Eng. Chem. Res.* vol. 50, pp.4441–4445.
5. Huang, B, Shao, H, Liu, N, Xu, ZJ & Huang, Y 2015, `From fish scales to highly porous N-doped carbon: a low cost material solution for CO₂ capture`, *RSC Adv.* vol. 5, pp. 88171–88175.
6. Lu, Y, Xiao, S, Gao, R, Li, J, & Sun, Q, 2014, `Improved weathering performance and wettability of wood protected by CeO₂ coating deposited onto the surface`, *Holzforschung*; vol. 68 no. 3, pp. 345–351.
7. Markovski, JS, Dokić, V, Milosavljević, M, Mitrić, M, Perić-Grujić, AA, Onjia, AE & Marinković, AD, 2014, `Ultrasonic assisted arsenate adsorption on solvothermally synthesized calcite modified by goethite, α -MnO₂ and goethite/ α -MnO₂`, *Ultrason. Sonochem.* vol. 21, pp. 790-801
8. Periyat, P, Laffir, F, Tofail, SAM, Magner, E & Facile A 2011, `Aqueous Sol–Gel Method For High Surface Area Nanocrystalline`, CeO₂, *RSC Adv.* vol. 1, pp. 1794-1798.
9. Sawana, R, Somasundar, Y, Iyer, VSh & Baruwati, B 2017, `Cerium modified activated carbon: an efficient arsenic removal adsorbent for drinking water purification`, *Appl. Water Sci.* vol. 7, pp. 1223–1230.
10. Taleb, K, Markovski, J, Veličković, ZS, Rusmirović, J, Rančić, M, Pavlović, V & Marinković, AD, 2016a, `Arsenic removal by magnetite-loaded amino modified nano/microcellulose adsorbents: Effect of functionalization and media size`, *Arab. J. Chem.*, DOI:<http://dx.doi.org/10.1016/j.arabjc.2016.08.006>,
11. Taleb, K, Rusmirović, J, Rančić, M, Nikolić, J, Drmanić, S, Veličković, Z & Marinković, A, 2016b, `Efficient pollutants removal by amino-modified nanocellulose impregnated with iron oxide`, *J. Serb. Chem. Soc.*, vol. 81, pp 1199–1213.
12. Veličković, ZS, Marinković, AD, Bajić, Z, Marković, J, Perić-Grujić, AA, Uskoković, PS & Ristić, MĐ, 2013, `Oxidized and Ethylenediamine-Functionalized Multi-Walled Carbon Nanotubes for the Separation of Low Concentration Arsenate from Water`, *Sep. Sci. and Techn.* vol. 48, pp. 2047-2058.
13. Veličković, ZS, Vuković, GD, Marinković, AD, Moldovan, MS, Perić-Grujić, AA, Uskoković, PS & Ristić, MĐ, 2012, `Adsorption of arsenate on iron(III) oxide coated ethylenediamine functionalized multiwall carbon nanotubes`, *Chem. Eng. J.* vol. 181-182, pp. 174-181.